

Dielectric and ferroelectric properties of $\text{Ba}(\text{Zr}_x\text{Ti}_{1-x})\text{O}_3$ ceramics

N. Nanakorn, P. Jalupoom, N. Vaneesorn, A. Thanaboonsombut*

*National Metal and Materials Technology Center, National Science and Technology Development Agency,
114 Thailand Science Park, Paholyothin Road, Klong Luang, Pathumthani 12120, Thailand*

Available online 4 October 2007

Abstract

It is known that Curie temperature of barium titanate system can be altered by the substitution of dopants into either A- or B-site. Dopants could pinch transition temperature, lower Curie temperature, and raise the rhombohedral–orthorhombic and orthorhombic–tetragonal phase transition close to room temperature. This isovalent substitution could improve the ferroelectric properties of the BaTiO_3 -based system. In this study, barium zirconate titanate $\text{Ba}(\text{Zr}_x\text{Ti}_{1-x})\text{O}_3$ (BZT; $x = 0, 0.02, 0.05$ and 0.08) ceramics were prepared by conventionally mixed-oxide method. The ferroelectric properties of BZT ceramics were investigated. Increasing Zr content in the BaTiO_3 -based compositions caused a decrease in Curie temperature (T_c). At T_c , the highest relative permittivity of BZT with an addition of 0.08 mol\% of Zr was 12,780. The BZT specimens with the additions of 0.05 mol\% and 0.08 mol\% of Zr presented the remanent polarization at $25 \mu\text{C}/\text{cm}^2$ and $30 \mu\text{C}/\text{cm}^2$, respectively.

© 2007 Elsevier Ltd and Techna Group S.r.l. All rights reserved.

Keywords: C. Dielectric properties; C. Ferroelectric properties; D. ZrO_2 ; BaTiO_3

1. Introduction

Barium titanate (BaTiO_3) is one of the most studied ferroelectric materials due to excellent properties, high dielectric constant [1,2] and low loss characteristics [3]. At the Curie temperature of 120°C , the crystal structure of BaTiO_3 changes from tetragonal to cubic accompanied by a sharp peak of the relative permittivity. For the ABO_3 perovskite, substituting A and/or B cation site by isovalent ions can alter electric behavior of the materials, e.g., the addition of strontium (Sr) into barium (Ba) site or hafnium (Hf) into titanium (Ti) site in barium titanate [4].

Recently, $\text{Ba}(\text{Zr}_x\text{Ti}_{1-x})\text{O}_3$ (BZT) has been chosen in the fabrications of ceramic capacitors because Zr^{4+} is chemically more stable than Ti^{4+} [5]. Moreover, Zr-substitution at Ti-site has been found to be an effective way to decrease the Curie temperature and exhibited several interesting features in the dielectric behavior of BaTiO_3 ceramics. Investigation has shown that the phase transition behavior of $\text{Ba}(\text{Ti}, \text{Zr})\text{O}_3$ materials can be changed from a normal phase transition to diffusive and further become a relaxor phase transition. The

modified BZT has shown systematic variations in the dielectric, piezoelectric and phase transition characteristics in the ceramics [5].

In perovskite structure, the relaxor behavior mainly occurs in lead-based compositions, e.g., lead magnesium niobate (PMN), lead scandium niobate (PSN), lead lanthanum zirconium titanate (PLZT), however, the diffuse phase transition, indicating the relaxor behavior, could occur in some particular compositions of lead-free piezoelectric ceramics, e.g., the barium zirconium titanate [6]. In this work, $\text{Ba}(\text{Zr}_x\text{Ti}_{1-x})\text{O}_3$ (BZT; $x = 0, 0.02, 0.05$ and 0.08) ceramics were prepared by a solid-state reaction method. The influence of Zr content on the dielectric and ferroelectric properties of the BZT ceramics with $0 \leq x \leq 0.08$ were examined and the results were discussed.

2. Experimental procedure

$\text{Ba}(\text{Zr}_x\text{Ti}_{1-x})\text{O}_3$ (BZT) ceramics were prepared via conventionally mixed-oxide method. The starting materials barium carbonate (BaCO_3) (98.5% Fluka), titanium dioxide (TiO_2 : rutile 99.0% Alfa Aesar) and zirconium oxide (ZrO_2 : <5 micron 99% Aldrich) were weighed based on the stoichiometric compositions of $\text{Ba}(\text{Zr}_x\text{Ti}_{1-x})\text{O}_3$ with $x = 0, 0.02, 0.05$ and 0.08 , respectively. The weighed batches were ball-milled in

* Corresponding author. Tel.: +66 2 564 6500x4240; fax: +66 2 564 6447.

E-mail address: areeh@mtec.or.th (A. Thanaboonsombut).

acetone for 24 h. After drying, the powders were calcined at temperatures ranging from 1150 °C to 1250 °C for 2 h. The calcined powders were again ball-milled in absolute ethanol for 24 h, dried and pressed into disks with a diameter of 20 mm and CIP at 2.5×10^8 N/m² for 10 min. The pellets were sintered at temperatures ranging from 1300 °C to 1450 °C for 2 h. Phase development and crystallographic structure of the ceramics were examined by X-ray diffraction analysis (JEOL, JDX-3530). The bulk densities of sintered samples were measured using Archimedes method, ASTM C 373-88. The suitable bulk densities of the sintered ceramics should reach 95–96% of the theoretical densities. Dried-silver paste was painted on both sides of the samples for dielectric and ferroelectric measurements.

The capacitances of the samples were measured using a 4194A Impedance Gain/Phase analyzer (Hewlett Packard) from 1 kHz to 1 MHz at the temperature range of –60 °C to 140 °C with a heating/cooling rate of 3 °C/min. The hysteresis loops were measured in temperatures ranging from 30 °C to 120 °C using RT66A Standardized Ferroelectric Measurement Test System (Radiant Technology).

3. Results and discussion

3.1. Densification of sintered BZT ceramics

Optimal sintering temperatures were chosen for their ability to reach the highest density comparable to the theoretical densities. The suitable sintering condition for the BZT ceramics with $x = 0$ and 0.02 was designed as 1300 °C for 2 h whereas that for the BZT ceramics with $x = 0.05$ and 0.08 was designed as 1400 °C for 2 h. At the optimum conditions (Fig. 1), the bulk densities of BZT-based specimens were insignificantly changed with the small amounts of Zr additives (less than 8 mol%). The densities of the BZT-based specimens were in the range of 95% of the theoretical density of the specimens.

3.2. Crystal structure of BZT ceramics

XRD patterns of BZT ceramics with $x = 0$, and 0.02 sintered at 1300 °C and $x = 0.05$ and 0.08 sintered at 1400 °C are shown in Fig. 2. As revealed from the XRD patterns, all BZT sintered ceramics had perovskite structure, indicating that the tetragonal phase of all BZT ceramics could be developed. Moreover, it

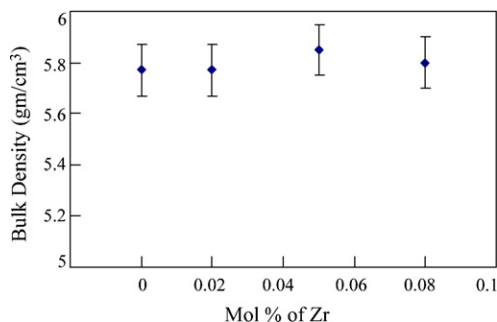


Fig. 1. Bulk density of sintered Ba(Zr_xTi_{1-x})O₃ ceramics as a function of x .

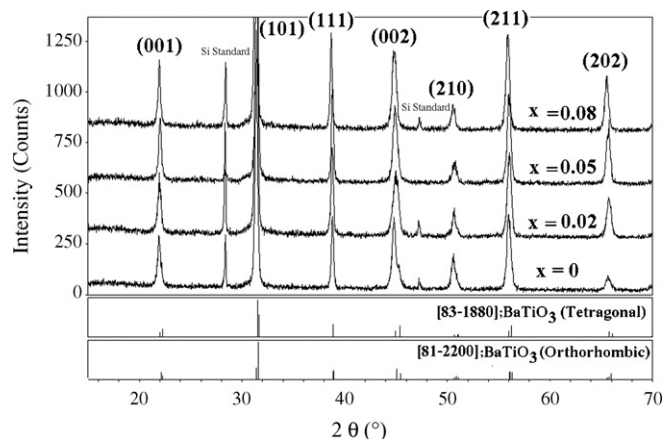


Fig. 2. XRD patterns of the BZT ceramics with $x = 0$, and 0.02 sintered at 1300 °C and $x = 0.05$ and 0.08 sintered at 1400 °C.

was observed that the diffraction peaks shifted to a lower angle with an increase in Zr content. Due to the fact that the ionic radius of Zr⁴⁺ (0.72 Å) is larger than that of Ti⁴⁺ (0.605 Å), thus, the substitution of Ti⁴⁺ by Zr⁴⁺ could increase the lattice parameter of ceramics [5].

3.3. Temperature dependence of relative permittivity

Fig. 3 shows the relative permittivity of BZT specimens with a change in temperatures at 1 kHz, 10 kHz and 100 kHz. The BZT ceramics with $x = 0$, 0.02 and 0.05 exhibited abrupt changes in relative permittivities about the region of 1st and 2nd phase transitions presenting a normal ferroelectric behavior. Moreover, it was observed that T_c shifted towards a higher temperature with an increase in the measured frequency (Fig. 3). With the addition of 8 mol% of Zr, the diffuse phase transition about Curie maxima occurred. This phenomena would be discussed in the following.

The transition temperature from orthorhombic to tetragonal structure (T_1) is observed as shown in Fig. 3. It is found that with increasing Zr content (0–5 mol%), the transition temperatures from tetragonal to orthorhombic structure shifts toward higher temperatures. Transition temperatures from orthorhombic to rhombohedral (T_2) are clearly shown only at $x = 0.05$. At $x = 0.08$, the diffuse phase transition occurs resulting in an unclear phase transition temperature (T_1 and T_2). The transition temperatures and Curie temperatures of the BZT-based compositions were recorded and summarized at Table 1. It should be concluded that the substitution of Zr in BZT-based system causes the shift in transition temperatures and the diffuse phase transition.

3.4. Ferroelectric behavior of BZT ceramics

Hysteresis loops (P versus E) measured at various temperatures are shown in Figs. 4–6 and summarized in Table 2. It should be noted that the pure BaTiO₃ (BT) specimens sintered at 1300 °C showed an antiferroelectric behavior at room temperature. This antiferroelectric phenomena of the pure BT specimens has been under-investigated for

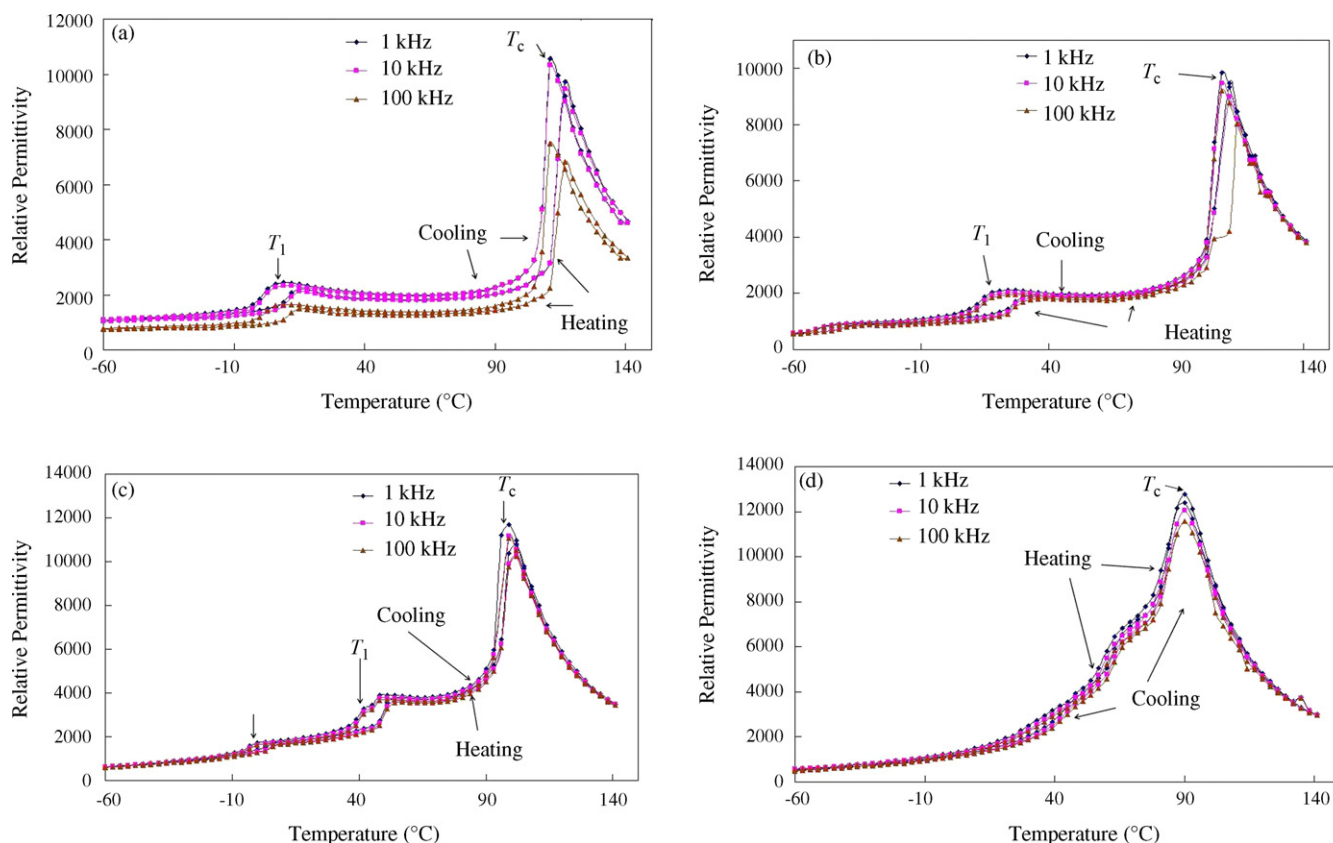


Fig. 3. Temperature dependence of the relative permittivity for $\text{Ba}(\text{Zr}_x\text{Ti}_{1-x})\text{O}_3$ ceramics with (a) $x = 0$ sintered at 1300°C , (b) $x = 0.02$ sintered at 1350°C , (c) $x = 0.05$ sintered at 1450°C and (d) $x = 0.08$ sintered at 1400°C at 1 kHz, 10 kHz and 100 kHz.

Table 1

The phase transition temperature (T_c , T_1 , T_2) maximum measured in BZT ceramics at 1 kHz

$\text{BaZr}_x\text{Ti}_{1-x}\text{O}_3$	T_1 ($^\circ\text{C}$)	T_2 ($^\circ\text{C}$)	T_c ($^\circ\text{C}$)
$x = 0.00$	6	–	117
$x = 0.02$	18	–	111
$x = 0.05$	42	0	102
$x = 0.08$	–	–	90

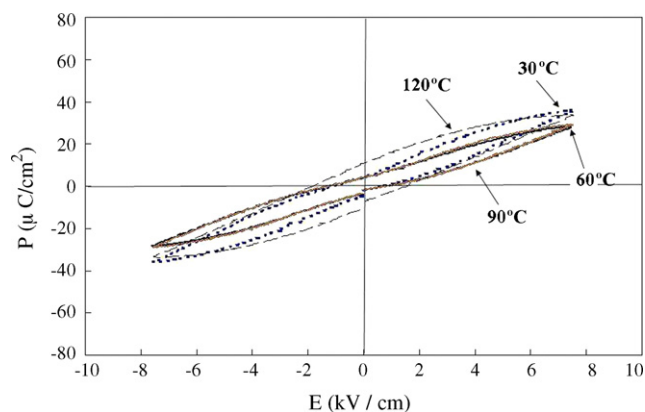


Fig. 4. Polarization vs. electric field at the temperatures ranging from 30°C to 120°C of $\text{BaZr}_x\text{Ti}_{1-x}\text{O}_3$ with $x = 0$ sintered at 1300°C .

further information. In addition, the P – E hysteresis loops of the pure BT specimens did not change with an increase in temperature. However, at the temperature of 120°C near the Curie temperature, the P – E hysteresis loop presented an elliptic shape. The similar behavior occurred with other BZT-based compositions when the specimens were measured at the temperature of 120°C . The P – E hysteresis loops of BZT specimens with $x = 0.05$ and 0.08 were decreased with an increase in temperature due to phase transition from ferroelectric to paraelectric (near T_c of ceramics). At 30°C , the BZT specimens with $x = 0.05$ and 0.08 exhibited remanent polarizations (P_r) at $25\ \mu\text{C}/\text{cm}^2$ and $29\ \mu\text{C}/\text{cm}^2$ and coercive fields (E_c) at $1.048\ \text{kV}/\text{cm}$ and $1.344\ \text{kV}/\text{cm}$, respectively.

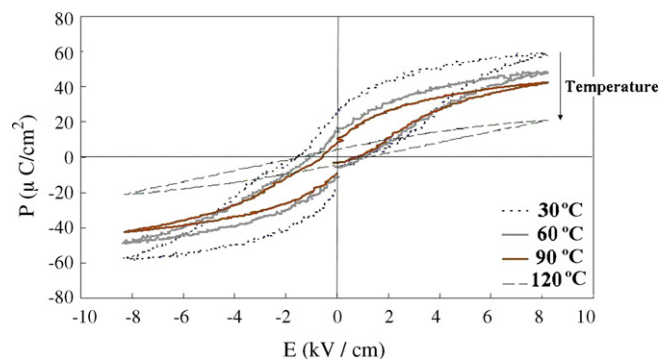


Fig. 5. Polarization vs. electric field at the temperatures ranging from 30°C to 120°C of $\text{BaZr}_x\text{Ti}_{1-x}\text{O}_3$ with $x = 0.05$ sintered at 1400°C .

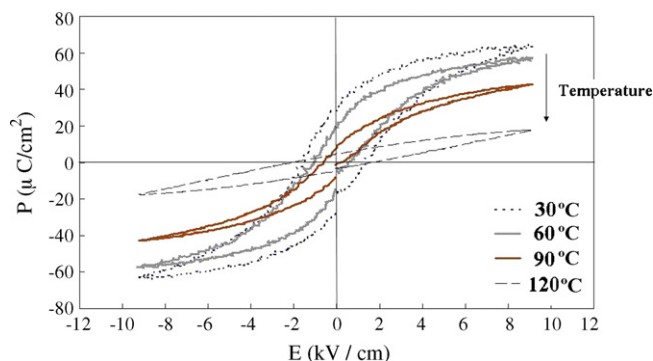


Fig. 6. Polarization vs. electric field at the temperatures ranging from 30 °C to 120 °C of $\text{BaZr}_x\text{Ti}_{1-x}\text{O}_3$ with $x = 0.08$ sintered at 1400 °C.

Table 2

The saturated polarization (P_s), remnant polarization (P_r), and coercive field (E_c) of BZT ceramics at 30 °C

$\text{BaZr}_x\text{Ti}_{1-x}\text{O}_3$	P_s ($\mu\text{C}/\text{cm}^2$)	P_r ($\mu\text{C}/\text{cm}^2$)	E_c (kV/cm)
$x = 0.00$	35.862	4.424	0.696
$x = 0.02$	12.324	2.143	0.912
$x = 0.05$	57.920	25.033	1.048
$x = 0.08$	63.320	29.451	1.344

4. Conclusions

The $\text{Ba}(\text{Zr}_x\text{Ti}_{1-x})\text{O}_3$ ceramics prepared by conventionally mixed-oxide method. The optimal sintering conditions for the BZT ceramics with $x = 0$ and 0.02 and the ones with $x = 0.05$

and 0.08 were designed as 1300 °C for 2 h and 1400 °C for 2 h, respectively. It was found that the Curie temperatures of the modified BZT compositions decreased with an increase in Zr content. The BZT-based ceramics with $x = 0.05$ and 0.08 showed the ferroelectric behavior and the maximum remanent polarization were 25 $\mu\text{C}/\text{cm}^2$ and 29 $\mu\text{C}/\text{cm}^2$, respectively.

Acknowledgement

This work is supported by National Metal and Materials Technology Center (MTEC), Thailand under the in-house project No. MT-B-48-CER-07-186-I.

References

- [1] Z. Yu, R. Guo, A.S. Bhalla, Dielectric behavior of $\text{Ba}(\text{Ti}_{1-x}\text{Zr}_x)\text{O}_3$ single crystals, *J. Appl. Phys.* 88 (2000) 410–415.
- [2] J. Zhao, L. Li, Y. Wang, Z. Gui, dc bias properties of $\text{Ba}(\text{Ti}_{1-x}\text{Zr}_x)\text{O}_3$ ceramics, *Mater. Sci. Eng. B99* (2003) 207–210.
- [3] B.D. Stojanovic, C.R. Foschini, V.B. Pavlovic, V.M. Pavlovic, V. Pejovic, J.A. Varela, Barium titanate screen-printed thick films, *Ceram. Int.* 28 (2002) 293–298.
- [4] H.Y. Tian, Y. Wang, J. Miao, H.L.W. Chan, C.L. Choy, Preparation and characterization of hafnium doped barium titanate ceramics, *J. Alloys Compd.* 431 (2007) 197–202.
- [5] B.L. Cheng, C. Wang, S.Y. Wang, H. Lu, Y.L. Zhou, Z.H. Chen, G.Z. Yang, Dielectric properties of $(\text{Ba}_{0.8}\text{Sr}_{0.2})(\text{Zr}_x\text{Ti}_{1-x})\text{O}_3$ thin films grown by pulsed-laser deposition, *J. Eur. Ceram. Soc.* 25 (2005) 2295–2298.
- [6] X.G. Tang, K.-H. Chew, H.L.W. Chan, Diffuse phase transition and dielectric tunability of $\text{Ba}(\text{Zr}_y\text{Ti}_{1-y})\text{O}_3$ relaxor ferroelectric ceramics, *Acta Mater.* 52 (2004) 5177–5183.